Petroleum Research 11 (2026) 501–515

Contents lists available at ScienceDirect

Petroleum Research

journal homepage: http://www.keaipublishing.com/en/journals/petroleum-research/

Full Length Article

Research on intelligent kick early warning technology based on LSTM-AE unsupervised learning

Boyuan Li[a,*], Zhaoxue Guo[a], Xudong Wang[a], Gui Tang[b], Xing Zuo[b]

[a] *Petroleum Engineering School, Southwest Petroleum University, Chengdu, 610500, Sichuan, China*
[b] *CNPC Chuanqing Drilling & Production Engineering Technology Research Institute, Sichuan, China*

A R T I C L E I N F O

Article history:
Received 31 July 2024
Received in revised form
28 September 2025
Accepted 21 October 2025
Available online 25 October 2025

Keywords:
Early kick warning
Drilling safety
Autoencoder
Machine learning
Downhole accident

A B S T R A C T

In oil and gas exploration, kick is a typical high-risk downhole incident. Currently, most intelligent kick detection methods belong to supervised learning, which depends on labeled samples and is prone to class imbalance issues in the training set, leading to reduced model accuracy and higher false alarm rates in practical applications. To address this, this paper focuses on the application of unsupervised learning in kick detection, proposing a kick detection method based on Long Short-Term Memory Autoencoder (LSTM-AE) combined with parameter trend change rules. The study integrates LSTM-AE with expert knowledge to develop an intelligent kick early warning system suitable for well sites, validated using field data from five wells. The results show that the average reconstruction mean squared error of the LSTM-AE is 0.017, with an average false alarm rate of 4.56% for kick detection, detecting kicks an average of 9.2 min earlier than manual detection. This outcome confirms that kick detection can utilize unsupervised learning methods, avoiding relying on labeled samples and class imbalance issues in the training set, thereby effectively improving model accuracy and generalization ability. Moreover, the proposed LSTM-AE demonstrates superior performance in kick detection, and the detection method combining the model and judgment rules has significant implications for monitoring and early warning of other types of downhole incidents.

1. Introduction

As oil and gas exploration and development continue to advance, deep earth exploration has become a crucial direction for further exploration in the petroleum industry. The deep earth domain is rich in oil and gas resources, characterized by challenging geological conditions such as deep burial, multiple stratigraphic layers, and complex pressure systems (Tan et al., 2024). In such a high-risk environment, drilling, as a long-cycle operation, is prone to frequent downhole accidents, with kick issues being particularly prominent. If not promptly addressed, kick can escalate into major safety incidents such as blowouts, resulting in significant losses to personnel and the economy. A typical case is the blowout accident at the Macondo well, which resulted in losses exceeding 14 billion dollars. Additionally, Mason (2019) analyzed spill incidents over the past two decades, revealing that as drilling depth increases, the likelihood of blowout accidents occurring also increases. Therefore, in the drilling process, there is an urgent need to adopt advanced kick detection technologies to monitor drilling data in real-time. This would enable the rapid and accurate detection of kick, reducing the probability and impact of such incidents.

In traditional operations, kick detection methods are mainly divided into surface parameter detection and downhole parameter detection. For example, the mud pit level detection method (Zhu et al., 2019), the inlet and outlet flow difference method (Ahmed et al., 2016), the standpipe pressure detection and casing pressure analysis method (Yang et al., 2019), and pulse detection technology using the Doppler effect (Fu et al., 2015). These methods monitor drilling data at the wellhead, but they suffer from issues such as data update delays, low accuracy, and frequent false alarms. With the widespread application of smart drillpipe monitoring (SDM) technology and measurement while drilling (MWD) technology, sensors can be installed on the drill string or near the drill bit to collect downhole data (Nayeem et al., 2016; Islam et al., 2017), and

* Corresponding author.
E-mail address: asd2000120@outlook.com (B. Li).
Peer review under the responsibility of Editorial Office of Petroleum Research.

https://doi.org/10.1016/j.ptlrs.2025.10.002
2096-2495/

mathematical and physical models can be used for simulation calculations to achieve early detection of kicks (Sun et al., 2018; Li et al., 2022; Su et al., 2024). Additionally, a method for kick and loss monitoring based on distributed fiber optic temperature measurement has been proposed. This method compares real-time measured temperatures with theoretically calculated temperatures to achieve kick monitoring (Zhang et al., 2023a). However, these traditional kick detection methods generally rely on high-precision level detectors, flow meters, and various sensors, which are expensive and challenging to operate normally in deep high-temperature and high-pressure environments. Therefore, in the face of complex geological environments, improving kick detection efficiency and reducing the false alarm rate have become research hotspots in the field of drilling safety.

Hargreaves et al. (2001) and Ritchie et al. (2008) developed a rapid drilling risk detection system within the Bayesian probability framework. The system, driven by historical data and expert knowledge, achieved the detection of complex downhole incidents, demonstrating the feasibility of using artificial intelligence (AI) technology for monitoring and risk identification in the drilling process. This provides new ideas and methods for safety management in drilling operations. In recent years, thanks to the development and application of AI in fault diagnosis and safety assessment technologies, research on intelligent detection and diagnosis of downhole drilling incidents has been further advanced. Kick detection has increasingly relied on AI technologies. In the early detection of kick accidents, intelligent kick detection methods based on expert systems have emerged. Fuzzy inference is one of the commonly used models in expert systems (Zhang, 2014; Zhang et al., 2016). This model utilizes expert knowledge and kick representation mechanisms, introduces a fuzzy rule base to construct kick knowledge base, and performs inference based on the characteristics of input parameters to achieve rapid and accurate kick detection. Some researchers have also utilized Bayesian Networks (BN) to develop expert systems for guiding engineers in safely completing operations such as well control and completion (Yue, 2014; Al-Yami et al., 2016). Although expert systems are capable of detecting kick and guiding safe operations, they rely on extensive knowledge bases built by experts, which can be confidential or expensive. To overcome reliance on expert knowledge, researchers have shifted their focus to utilizing vast amounts of historical drilling data. As a result, traditional machine learning methods such as K-nearest neighbors (KNN), clustering, decision tree, BN, and support vector machines (SVM) have been employed. Alouhali et al. (2018) utilized KNN for classifying surface measurement parameters to achieve kick detection. Sule et al. (2019) proposed a novel scheme for safety and reliability assessment of controlled pressure drilling operations, utilizing BN for reliability evaluation of kick control operations in dynamic annular pressure control systems. Nhat et al. (2020) utilized downhole historical data to create a kick detection model based on BN. Experimental results demonstrated the effectiveness of BN in kick detection, and the output results could be used as part of automatic well-control decisions. Li et al. (2023,b) employed an improved fuzzy C-means clustering based on relative entropy to cluster standpipe pressure and casing pressure, determining the occurrence of kick. Ge et al. (2023) established a random forest intelligent warning model for kick severity classification based on downhole annular parameters. Zhang and Chi (2023) established a kick risk assessment model using BSMOTE-SVM, improving kick identification capability in drilling operations. However, these traditional machine learning methods require manual feature selection and extraction, making model construction difficult and computation complex. Additionally, when handling large-scale data, they struggle to capture the complex relationships between data points, and cannot fully learn the features and patterns in the data.

The world is currently in the era of Industry 4.0, where data-driven fault detection and diagnosis techniques, reliability assessment, and accident control management are becoming mainstream research directions (Arunthavanathan et al., 2021). The main topic has become how to build a large-scale drilling database and how to fully utilize massive historical data (Osarogiagbon et al., 2021). There has been a noticeable trend toward the use of deep learning. In kick detection, Yin et al. (2014) constructed a real-time kick warning model using backpropagation neural network (BP) and applied it in the DS01 well in the Sichuan Basin. Muojeke et al. (2020) explored whether the simplest artificial neural network could detect kick. The study indicated that a simple feedforward neural network could detect kick, but to distinguish between various abnormal drilling events, a more complex neural network structure was required. Zhao et al. (2022) employed k-means clustering to process data and utilized recurrent neural networks (RNN) for kick detection. Although these simple models can achieve kick detection and exhibit certain robustness, they may fall into local optima and have slow training convergence and a tendency to overfit when dealing with high-dimensional data. Some researchers attempted to address the limitations of simple models by adding optimization functions. Xie et al. (2018) optimized network parameters using a genetic algorithm (GA) to mitigate the shortcomings of simple models. They developed a genetic wavelet ANN kick detection model, which improved the accuracy of kick detection. Li (2021) compared the performance of three models: BP, GA-BP, and CPSO-BP. The study showed that models incorporating optimization functions, such as GA-BP and CPSO-BP, outperformed the BP model. While these optimized models indeed improved detection accuracy, they overlooked the temporal characteristics of drilling data, resulting in no significant advantage in early detection. To achieve early detection, models capable of effectively handling time series problems such as LSTM and GRU have been applied. Fjetland et al. (2019) utilized an LSTM model to detect and predict the scale of formation fluid influx during drilling processes. Wang et al. (2022), b proposed an adaptive LSTM kick warning model, achieving adaptive feature extraction for different well data and improving model versatility. Xu et al. (2023) achieved quantitative prediction of drilling risk profiles using a trained LSTM model and calculations of virtual well-related parameters. Sun et al. (2023) proposed an intelligent monitoring method for kick and loss combining drilling conditions with BiGRU, resulting in lower false alarm rates compared to BiGRU without considering drilling conditions. Zhang et al. (2023) implemented hierarchical warning for kick using a cascade GRU model, resulting in earlier warning times compared to traditional GRU models. These models have achieved significant improvements in early prediction, but there are still some shortcomings. To reduce the risk of single model failure, improve model identification performance and generalization ability, and enhance model reliability, hybrid models combining multiple models or techniques have been applied. Osarogiagbon et al. (2020) utilized an LSTM-RNN model to capture the temporal relationship between the D-index and standpipe pressure combination data, achieving early kick detection. Kopbayev et al. (2022) combined CNN and BiLSTM for fault detection and diagnosis, and this hybrid model showed promising results in early leakage detection in natural gas facilities. Wang et al. (2023) employed LSTM-RNN to individually predict several sensitive kick indicators and constituted a strong learner using ensemble learning, achieving accurate kick detection with detection speeds surpassing some common methods in the industry. Wang et al. (2022),b constructed models using RUSboosted, Subspace-KNN, and BaggedTree algorithms and employed ensemble learning for gas invasion detection, with ensemble learning predicting errors below 10% in most cases. These hybrid models and novel approaches allow for effective information provision from other models when a single model encounters issues, thus mitigating safety risks and ensuring the smooth operation of drilling projects. Yin et al. (2023) also proposed the application of Seq2Seq and Informer models with attention mechanisms in early kick detection. In recent years, machine learning methods based on mechanism constraints and big data integration have become an important research direction in the petroleum field. For example, researchers have developed intelligent kick detection tools that improve model accuracy by combining physical modeling with Bayesian networks (Andia et al., 2018), big data analysis with formation modeling (Isemin et al., 2019), and fluid mechanics with ANN (Obi et al., 2022; Shi et al., 2023). Additionally, training methods using hybrid physical data (Li et al., 2023; Zhang and Samuel, 2024) and physics-constrained distributed neural networks (Ma et al., 2024) have further enhanced model accuracy and interpretability.

From publicly published research results, it can be seen that in the development of intelligent kick detection methods, widely adopted expert systems, traditional machine learning algorithms, and deep learning models predominantly use supervised learning. These methods rely on labeled samples, which entail high annotation costs, suffer from class imbalance in the training set, and exhibit low model generalization capabilities. However, unsupervised learning has been widely applied in process safety and fault diagnosis tasks, as it can discover patterns and relationships from unlabeled data, making it well-suited for handling large datasets. For example, deep CNN-AE have been used for drill bit wear assessment (Agostini et al., 2020), OSAVA for fault detection in chemical processes (Bi and Zhao, 2021), RNN-AE for stuck pipe detection (Konda et al., 2022), and CNN-AE based automated well logging (Park and Jeong, 2023). Models based on autoencoders can identify anomalies by learning the patterns and relationships of normal data.

Therefore, this paper proposes an intelligent kick detection method based on unsupervised learning. This method comprises two parts: 1) anomaly detection in the drilling process based on the LSTM-AE model. 2) kick determination guided by parameter trend change rules. The intelligent kick early warning system constructed using this method enables early kick detection, verifies the effectiveness of unsupervised learning in kick detection, eliminates dependence on labeled datasets, and avoids the class imbalance issue caused by the scarcity of kick samples. This method was applied using field data from five wells, demonstrating its effectiveness and reliability in enhancing drilling process safety and risk control.

The rest of the paper is organized as follows. Section 2 details the procedural steps and theoretical framework of the proposed method in sequential order. Section 3 presents the case study experiments and analysis of the method. Section 4 provides a summary of the paper.

2. Material and methods

2.1. Parameter selection

The comprehensive logging data in the well field covers numerous parameters, which can be broadly categorized as follows (Li, 2020): 1) directly measured parameters including casing pressure, hook load, in-out density, etc. 2) basic computational parameters such as in-out flow rates, drilling pressure, mud pit volume, etc. 3) analytical parameters involving shale density, ash content, etc. 4) other logging parameters such as cuttings logging, geochemical logging, etc. While a rich set of parameters is beneficial for accurate kick detection, it also makes data analysis more complex and increases the difficulty of feature extraction from high-dimensional data. In the field, when a kick occurs, the invasion of formation fluids causes significant changes in directly measured parameters and basic calculated parameters. Therefore, using a Pearson correlation coefficient heatmap to quantitatively analyze the correlation between these two types of parameters can help select the relevant parameters that are most indicative of a kick from among the numerous parameters. The Pearson correlation coefficient, based on statistical theory, is commonly used to describe the degree of correlation between data points. Its value ranges between -1 and 1. A value closer to -1 or 1 indicates a higher similarity in characteristics between the two parameters, while a value closer to 0 indicates a lower similarity. By using the correlation coefficient, a Pearson correlation coefficient matrix can be constructed and color-coded to create a heatmap. This heatmap visually represents the correlation characteristics between the two parameters, providing an intuitive description of their relationship. As shown in Fig. 1, ten parameters related to kick detection were selected for correlation analysis.

As shown in Fig. 1 and 1) the rate of penetration shows a strong negative correlation with the total pit volume and a strong positive correlation with torque and standpipe pressure. 2) The outlet flow rate shows a strong positive correlation with the total pit volume. 3) The inlet density is strongly positively correlated with both the outlet density and the total pit volume. 4) the outlet density also shows a strong positive correlation with the total pit volume. Using these strongly correlated parameters as inputs for the model allows it to learn more potential combined features, thereby enhancing the model's accuracy. However, relying solely on the Pearson correlation coefficient to select parameters lacks physical interpretation and may lead to discrepancies due to factors such as geological environment, external interference, and measurement instruments. For instance, there is no significant correlation between inlet/outlet density and total pit volume in reality. Therefore, further selection should be combined with kick characterization.

In the early characterization of kicks, changes in parameters such as standpipe pressure, torque, drill pressure, and rate of penetration are transient variations caused by abnormal formation pressure. These parameters tend to change earlier and exhibit rapid changes. On the other hand, parameters like hook load, outlet density, and total pit volume only start to change after formation fluids invade the wellbore, with abnormal fluctuations appearing later and changing more slowly. Additionally, when encountering a reservoir or anomalously high-pressure formations during drilling, issues such as formation under pressure, fractures, or cavern development can cause the drill bit to lose support, resulting in reduced drill pressure, a sudden increase in rate of penetration, and unstable fluctuations in torque. Furthermore, when formation fluids invade the wellbore, changes in drilling fluid properties affect the buoyancy of the drill string, which also leads to variations in drill pressure, rate of penetration, and torque. In complex geological environments, parameters like drill pressure, drilling rate, and torque can exhibit unstable changes due to different encountered formations. Therefore, to enable the model to effectively learn the characteristic patterns of parameters during a kick, these parameters are given lower priority.

Combining Pearson correlation coefficient analysis with kick characterization analysis, this paper selects standpipe pressure, total pit volume, hook load, outlet flow rate, and outlet density as the input parameters for the model. These five parameters maintain long-term stability during the drilling process, exhibit strong correlations, and show significant changes during a kick.

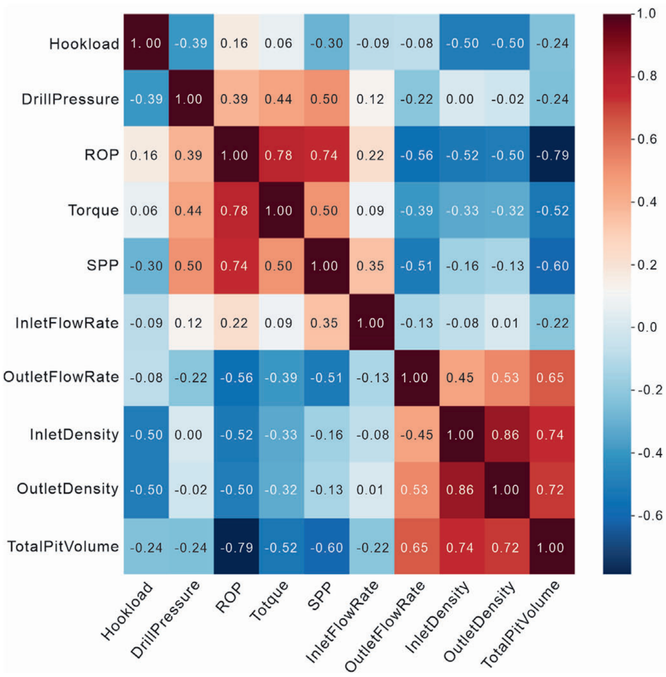

Fig. 1. The association feature map of kick related parameters.

2.2. Data preparation

Due to the impact of complex environments on the accuracy of measurement sensors, logging data contains anomalies that exhibit abrupt increases or decreases. These anomalies can significantly interfere with model accuracy, necessitating data cleaning to remove noise. As shown in the box plots in Fig. 2, anomalies are present in the parameters of hook load, outlet flow rate, and standpipe pressure.

In drilling data, normal data far exceeds abnormal data, and theoretically, anomalies could be directly removed. However, since drilling process data has time series characteristics, directly removing anomalies might affect the underlying features of the data. Therefore, this paper first uses a moving average filter to clean and optimize the data, eliminating noise, and then removes the anomalies. This approach minimizes interference with the model's accuracy to the greatest extent possible.

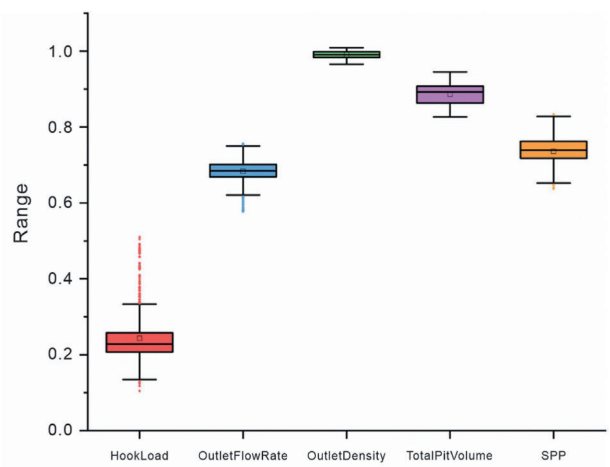

Fig. 2. Boxplot before data cleaning.

The moving average filter is a type of digital filter that can filter out high-frequency noise from sensor signals. Its mathematical expression is as follows:

$$(a*v)[n] = \sum_{m=-\infty}^{\infty} a[m]v[n-m] \tag{1}$$

where a is the input data (data to be processed); v is the convolution kernel; m is the index of the convolution kernel; n is the index of the input data. The filter can be viewed as a one-dimensional array that is convolved with the signal data to obtain the smoothed result. The specific convolution process can be seen in Fig. 3.

In the application of moving average filtering, the kernel size is typically selected based on a comprehensive consideration of data characteristics, signal-to-noise ratio, and system response time. A larger kernel is more effective in smoothing data with high-frequency noise or a high noise ratio, as it averages over a broader range of samples to suppress noise. In contrast, a smaller kernel is preferable when rapid system response is required. Considering the frequent and substantial fluctuations in drilling data, the need for timely kick detection, the 2-s sampling interval of the training data, and the reliance of the proposed method for kick detection on trend information, a kernel size of 10 was determined through empirical evaluation. Fig. 4 shows the results of raw data processed using a moving average filter with a kernel size of 10. This moving average filter effectively handles high-frequency noise.

Subsequently, anomaly removal is performed. The processed data no longer contains anomalies in hook load, outlet flow rate, and standpipe pressure, as shown in Fig. 5.

In summary, the data cleaning method and process described in this paper are effective, as they efficiently suppress data jitter, smooth the data, and maintain the accuracy, completeness, and validity of the data trends.

Before training the model, it is necessary to normalize the data to avoid the imbalance caused by different dimensions and units, which can accelerate the convergence speed and improve the robustness of the model. This paper uses min-max normalization to process the data, the specific formula is as follows:

$$\begin{cases} X_{std} = \dfrac{X - X.\min(axis = 0)}{X.\max(axis = 0) - X.\min(axis = 0)} \\ X_{scaled} = X_{std} \times (\max - \min) + \min \end{cases} \tag{2}$$

where X_{std} is the standardized result; X is the row vector; $X.\min(axis = 0)$ is the row vector consisting of the minimum values in each column; $X.\max(axis = 0)$ is the row vector consisting of the maximum values in each column; X_{scaled} is the normalized result; max is the maximum value of the mapping interval; min is the minimum value of the mapping interval. The data in Fig. 6 shows that normalization ensures uniformity of units across all parameters.

2.3. LSTM-AE model

Currently, research on intelligent kick identification treats the kick problem as a binary classification task, using datasets with kick and normal labels to train the model and classify new input data. This is done using supervised learning to identify kicks. However, drilling data is multivariate time series data with a large volume, and it exhibits nonlinear characteristics due to geological conditions, with kick data being extremely scarce. Additionally, the accuracy of field parameter measurements is relatively low, resulting in a significant amount of noise in the data. In such cases, the cost of

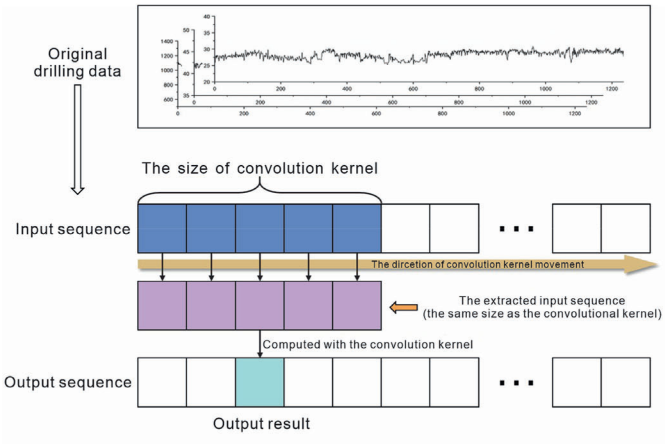

Fig. 3. The operational process of a sliding mean filter involves.

labeling kick data is high, making supervised learning methods that rely on labeled data impractical and ineffective for timely and accurate kick warnings. Therefore, this paper addresses the issue from the perspective of fault diagnosis, transforming kick detection from a binary classification problem into an anomaly detection problem. By incorporating the characteristics of kick events, further determination of kick is made on the anomalous sequences.

This paper proposes an LSTM-AE model based on the principle of autoencoders, which differs from the LSTM model used in classification tasks, as shown in Fig. 7. This model is a multivariate time series anomaly detection model capable of quickly and accurately identifying anomalous sequences in drilling data. It belongs to the category of unsupervised learning and does not rely on labeled datasets.

Instead, it utilizes normal data X for self-supervised learning, aiming to let the network learn a mapping relationship to output reconstructed data X^R that is as close as possible to the original input data.

In Fig. 7, LSTM-AE guides the neural network to learn a function:

$$\begin{cases} X^R = f_{W,b}(X) \approx X \\ W = \left\{W^{(1)}, W^{(2)}\right\} \\ b = \left\{b^{(1)}, b^{(2)}\right\} \end{cases} \tag{3}$$

where $W^{(1)}$ is the weights of the encoder; $W^{(2)}$ the weights of the decoder; $b^{(1)}$ is the bias of the encoder; $b^{(2)}$ the bias of the decoder. The process of mapping the raw data X from the input layer to the hidden layer is as follows:

$$o = \sigma\left(W^{(1)}X + b^{(1)}\right) \tag{4}$$

where o is the latent encoding of X after passing through the encoder; $\sigma(\cdot)$ is the activation function of the encoder. The process of mapping the latent encoding o from the hidden layer to the output layer is as follows:

$$X^R = \delta\left(W^{(2)}o + b^{(2)}\right) \tag{5}$$

where X^R is the reconstructed raw data; $\delta(\cdot)$ is the activation function of the decoder.

By minimizing the difference between the original data and the reconstructed data, the autoencoder can produce a small reconstruction error when reconstructing normal data and a large reconstruction error for abnormal data. This enables the identification of anomalous sequences. The LSTM layer (Greff et al., 2017), as shown in Fig. 8, has three gating units that combine information from the current time step and the previous time step, control parameter updates, and determine which information to retain. Compared to RNN, LSTM can address the issues of vanishing and exploding gradients in long-sequence training, making them perform better in longer sequence training.

Therefore, the encoder and decoder of the model are constructed using two-layer LSTM layers. The first layer extracts time series features from the input data, and the second layer uses these features for prediction and reconstruction, outputting latent representations and reconstructed data. Additionally, to limit the size of the weights, simplify the network structure, prevent overfitting, and improve the model's generalization ability, an L2 regularization term is added to the LSTM layers (He et al., 2019). This adds the sum of the squared weights to the loss function, achieving weight decay and smoothing the weights. The model also employs the Adam optimization algorithm as the optimizer, which is simple to implement, computationally efficient, and memory-efficient (Kingma and Ba, 2015). It can adaptively adjust the learning rate, improving the gradient descent process and allowing the neural network parameters to update based on gradient information during backpropagation. This minimizes the loss function and enhances the model's robustness. In terms of the choice of loss function, since the LSTM-AE model detects anomalous sequences based on reconstruction, the reconstruction mean squared error (MSE) is used:

$$Loss(MSE) = \frac{1}{n}\sum_{i=1}^{n}\left(X_i - X_i^R\right)^2 \tag{6}$$

The anomaly threshold d is determined by the kernel density estimation (KDE) of the calculated losses from the training set. This paper uses Gaussian kernel density estimation:

$$\begin{cases} \widehat{f}(x) = \dfrac{1}{nh}\displaystyle\sum_{i=1}^{n} K\left(\dfrac{x - x_i}{h}\right) \\ K(x) = \dfrac{1}{\sqrt{2\pi}}\exp\left(-\dfrac{x^2}{2}\right) \end{cases} \tag{7}$$

where x is the input value; $K(\cdot)$ is the Gaussian kernel function; n is the sample size; h is the bandwidth; $\widehat{f}(x)$ is the estimated probability density function at x. The threshold d for determining sequence anomalies is established based on the probability density distribution. If the calculated loss in the test set exceeds d, it is considered an anomaly.

2.4. Kick warning rules

Using the LSTM-AE model to identify drilling data can only detect anomalous sequences but cannot determine whether these anomalies indicate a kick. Therefore, it is necessary to perform trend analysis on individual parameters. Based on kick characterization analysis, when a kick occurs, certain parameters exhibit specific trends. The values of total pit volume (V_t), outlet flow rate (F_o), and hook load (H_n) gradually increase, while the values of outlet density (D_o) and standpipe pressure (S_m) gradually decrease. The original single-variable sequences of the five parameters are as follows:

$$\begin{cases} V_t = \{v(t_1), v(t_2), \cdots, v(t_n)\} \\ F_o = \{f(t_1), f(t_2), \cdots, f(t_n)\} \\ H_n = \{h(t_1), h(t_2), \cdots, h(t_n)\} \\ D_o = \{d(t_1), d(t_2), \cdots, d(t_n)\} \\ S_m = \{s(t_1), s(t_2), \cdots, s(t_n)\} \end{cases} \tag{8}$$

where $T = \{t_1, t_2, \cdots, t_n\}$ represents the set of corresponding time points. The reconstructed sequences of the data are as follows:

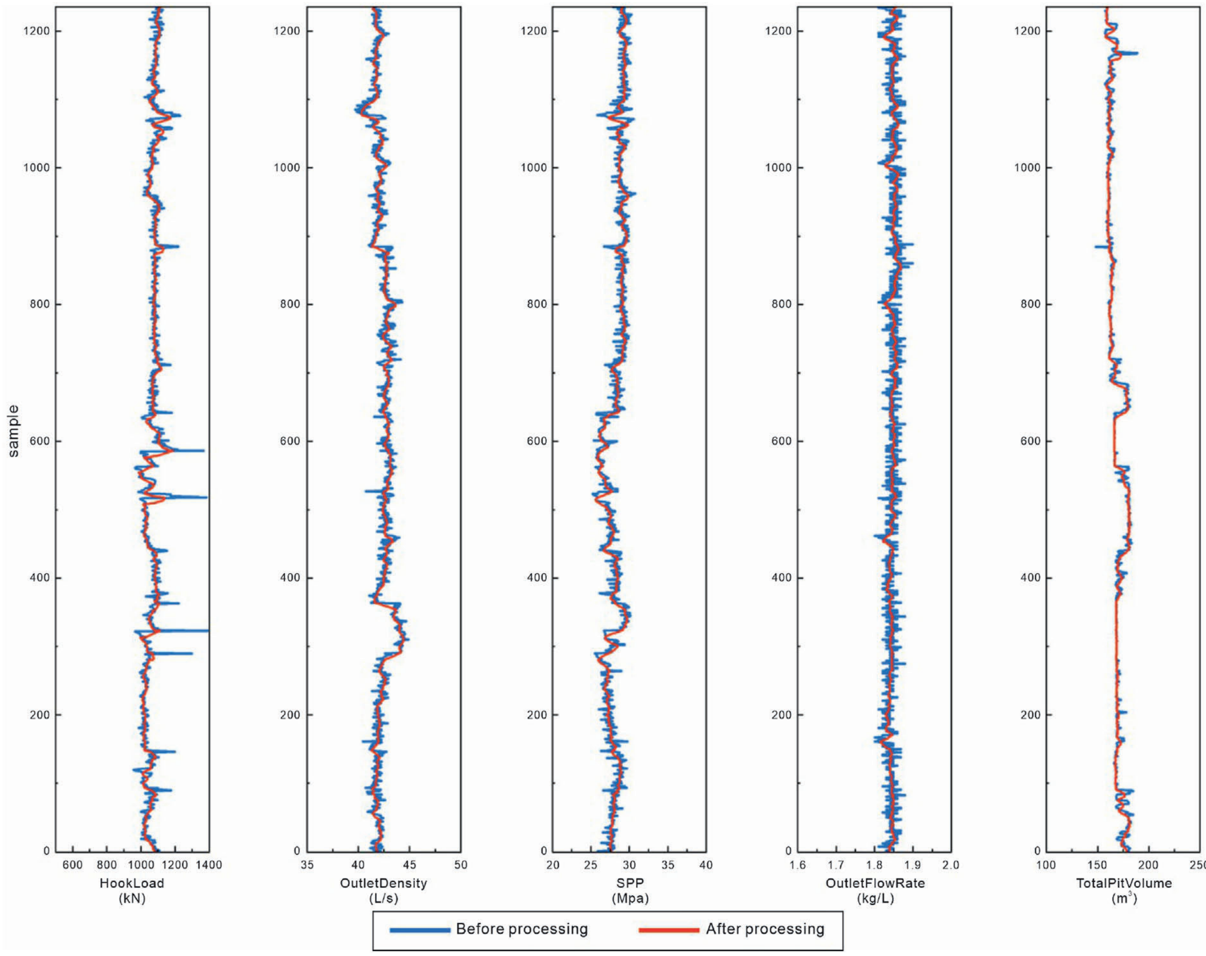

Fig. 4. Comparison graph before and after applying sliding mean filter.

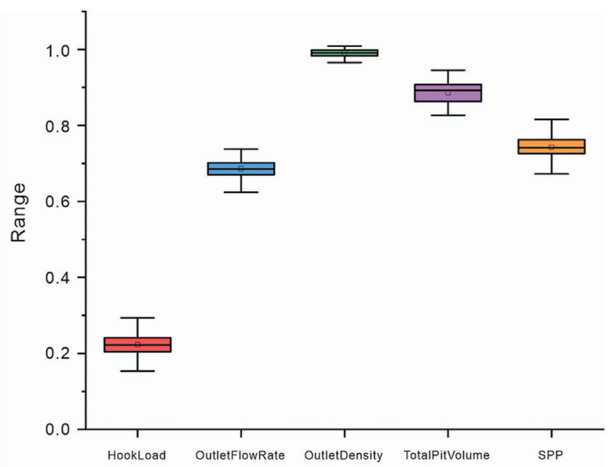

Fig. 5. Boxplot after data cleaning.

$$\begin{cases} \tilde{V}_t = \{\tilde{v}(t_1), \tilde{v}(t_2), \cdots, \tilde{v}(t_n)\} \\ \tilde{F}_o = \{\tilde{f}(t_1), \tilde{f}(t_2), \cdots, \tilde{f}(t_n)\} \\ \tilde{H}_n = \{\tilde{h}(t_1), \tilde{h}(t_2), \cdots, \tilde{h}(t_n)\} \\ \tilde{D}_o = \{\tilde{d}(t_1), \tilde{d}(t_2), \cdots, \tilde{d}(t_n)\} \\ \tilde{S}_m = \{\tilde{s}(t_1), \tilde{s}(t_2), \cdots, \tilde{s}(t_n)\} \end{cases} \tag{9}$$

When using an LSTM-AE trained with normal data to reconstruct abnormal sequences, the values of individual variables in the sequence tend to shift towards those of normal data. Therefore, when the abnormal sequence corresponds to the occurrence of kick, the reconstructed abnormal single-variable data will tend toward the normal drilling data. Using normal data as a reference, the trend change in abnormal data can only be either increased (with a value of 1) or decreased (with a value of -1). Hence, trend change rules can be formulated as follows:

1) If $\forall t \in T$, $v_t > \tilde{v}_t$, then $V = 1$; conversely, $V = -1$.
2) If $\forall t \in T$, $f_t > \tilde{f}_t$, then $F = 1$; conversely, $F = -1$.
3) If $\forall t \in T$, $h_t > \tilde{h}_t$, then $H = 1$; conversely, $H = -1$.
4) If $\forall t \in T$, $d_t > \tilde{d}_t$, then $D = 1$; conversely, $D = -1$.
5) If $\forall t \in T$, $s_t > \tilde{s}_t$, then $S = 1$; conversely, $S = -1$.

Different types of incidents exhibit distinct trends in various variables. By combining anomaly detection models with trend change rules and leveraging expert knowledge. The drilling process state can be classified into kick ($label = 1$), normal ($label = 0$), and other incidents ($label = -1$). The specific rules are as follows:

1) When $d < Loss$, and $V = F = H = 1$ and $D = S = -1$, then $label = 1$.
2) When $d < Loss$, and $V, F, H \neq 1$ or $D, S \neq -1$, then $label = -1$.
3) When $d > Loss$, then $label = 0$.

When the model detects an anomalous sequence, it calculates and analyzes the five individual variables reconstructed by the LSTM-AE model against the original anomalous data to determine

No.	HookLoad (kN)	TotalPitVolume (m³)	OutletFlowRate (L/s)	OutletDensity (kg/L)	SPP (MPa)
1	1109.10	180.29	41.82	1.83	27.24
2	1078.28	180.29	41.41	1.84	27.79
...	...	...	...	...	...
200	1049.06	168.43	42.07	1.84	27.11
201	1042.34	168.58	42.50	1.83	26.70
...	...	...	...	...	...

⇒

No.	HookLoad (kN)	TotalPitVolume (m³)	OutletFlowRate (L/s)	OutletDensity (kg/L)	SPP (MPa)
1	0.455	0.486	0.171	0.436	0.872
2	0.429	0.484	0.158	0.418	0.854
...	...	...	...	...	...
200	0.174	0.368	0.177	0.273	0.497
201	0.160	0.397	0.178	0.273	0.496
...	...	...	...	...	...

Fig. 6. The normalized result.

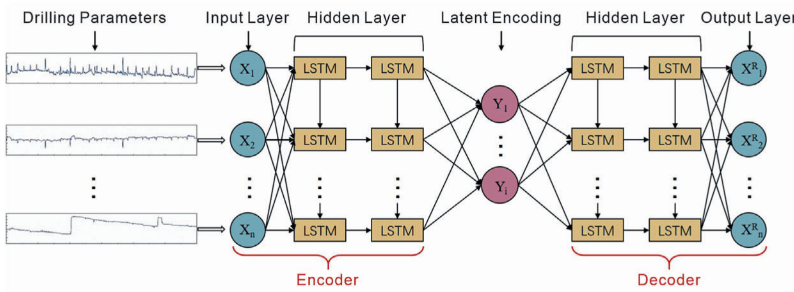

Fig. 7. The structure of the LSTM-AE model.

the trend changes of each parameter. Based on these trend changes, appropriate warning information is provided. The specific process is detailed in Fig. 9 and Table 1.

2.5. Warning system

In this study, the trained LSTM-AE model proposed in Section 2.3 and the kick early warning rules proposed in Section 2.4 are integrated to build an intelligent kick early warning system suitable for field application. The detailed structure of this system is shown in Fig. 10. This system will be utilized in the case study presented in Section 3.2.

The system consists of three parts. The first part is the database system, where surface measurement data and downhole measurement data are transmitted to and stored in the logging database at the well site after signal decoding. This database grants querying permissions to the model training server and client machines. The second part is the model training server, which periodically retrieves data from the logging database, provides datasets for model training and validation, and conducts LSTM-AE model training. The trained model and anomaly threshold data are then regularly transferred to client machines. The third part is the intelligent warning software deployed on client machines, allowing on-site

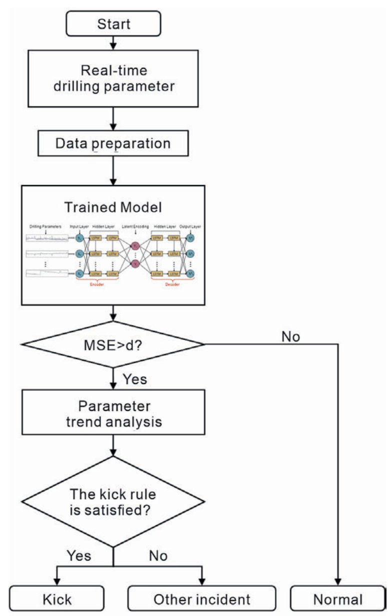

Fig. 9. The kick detection process.

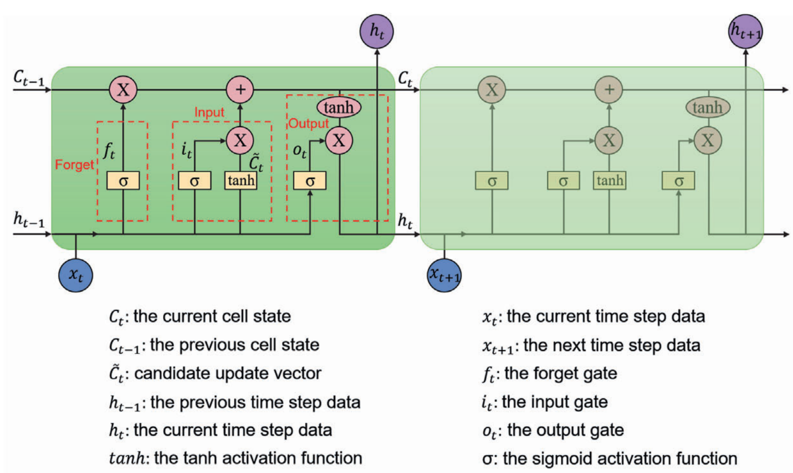

Fig. 8. The structure of the LSTM layer.

Table 1
The pseudo-code of early kick warning.

Algorithm: Early warning of Kick

Input: The training dataset X consists of a multivariate time series of normal drilling data, including mud pit volume (V_t), outlet flow rate (F_o), hook load (H_n), outlet density (D_o) and standpipe pressure (S_m). The online drilling data Y also includes the same parameters as the training dataset;
Output: The early warning result *label*;
Operation:

Train the LSTM-AE model using X and obtain reconstructed data X^R;
Calculate $Loss(MSE)$ using equation (6), and use equation (7) to compute and plot the probability density distribution of $Loss(MSE)$. Based on the distribution, determine the anomaly threshold d;
Utilize the trained LSTM-AE to reconstruct Y, and obtain the reconstructed data Y^R;
Calculate $Loss$ between Y and Y^R;
If $Loss < d$ **then**
  $label = 0$;
Drilling operation proceeds normally;
else
  Analyze each variable of the abnormal sequence according to the trend change rules;
  If $V = F = H = 1$ and $D = S = -1$ **then**
  $label = 1$;
  The abnormal sequence indicates kick;
else
  $label = -1$;
  The data segment exhibits significant fluctuations, potentially indicating other complex downhole incidents;
  end if
end if

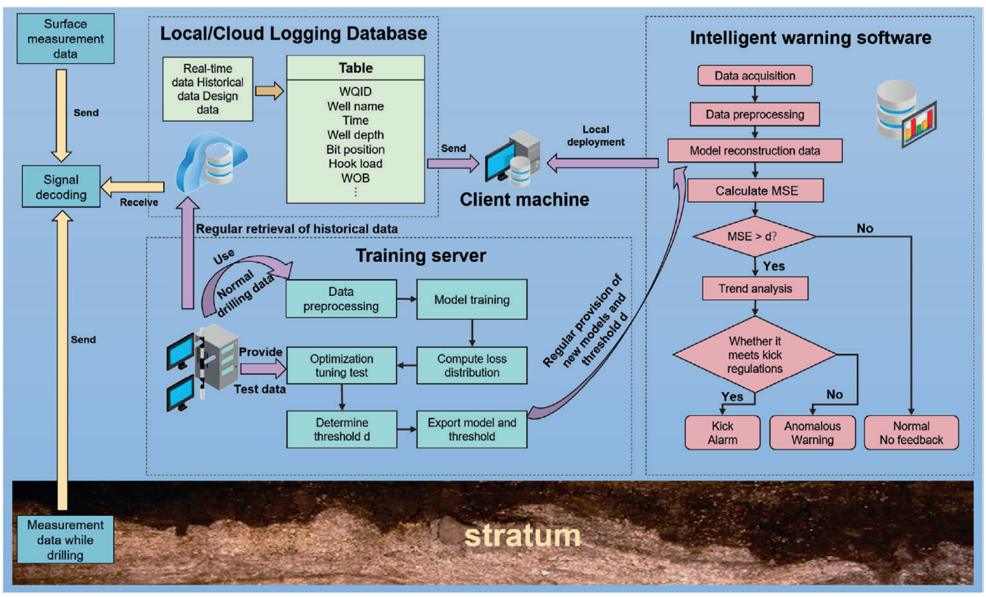

Fig. 10. The kick intelligent warning system.

personnel to selectively update or restore the models and thresholds of the client software. By running the software, real-time drilling data can be monitored for kick. Upon detecting anomalies or confirming kick, the software controls the alarm devices connected to the client machine, issuing corresponding levels of warning signals, and generating analysis reports and logs to provide decision-making and analysis basis for on-site personnel's abnormal disposal actions. Additionally, the software records the accuracy of the models and thresholds, providing feedback for model update training to ensure continuous improvement in performance and accuracy of the monitoring system.

3. Results and discussion

3.1. Model training

In this paper, the LSTM-AE model constructed consists of 7 layers. By adjusting the number of neurons in the LSTM layers and selecting the optimal batch size, we determine the optimal model parameters. The specific configuration parameters of the optimal LSTM-AE model selected in this paper are shown in Table 2, which will serve as the warning system model.

In this study, 28576 pieces of normal data, away from the kick section, were selected from 3 wells. These were divided into groups of 32 data samples each, resulting in a total of 893 groups. These groups were used to train the LSTM-AE configured as shown in Table 2. During model training, the optimization function used was Adam with a learning rate of 0.001. The training results are shown in Fig. 11, where the model converges at the 100th epoch.

Subsequently, the Gaussian kernel density estimation distribution of the training set loss was plotted, as shown in Fig. 12. This graph helps determine the appropriate threshold for anomaly detection. In this study, a threshold d of 0.20 was selected; any $Loss(MSE)$ in the test set higher than d is considered an anomaly.

Fig. 13 shows the anomaly detection results for a segment of drilling data with $d = 0.20$. The results indicate that out of 4913

Table 2
The configuration parameters of the LSTM-AE model.

No.	Parameters	Value
1	Number of layers	7 (Input layer、2 LSTM layers、Latent representation layer、2 LSTM layers、Output layer)
2	Neurons per layer	5、16、4、4、4、16、5
3	Activation function	Relu
4	Optimization algorithm	Adam
5	Loss function	MSE
6	Maximum Epoch	100
7	Batch size	32
8	Data partitioning	80% training set, 20% test set

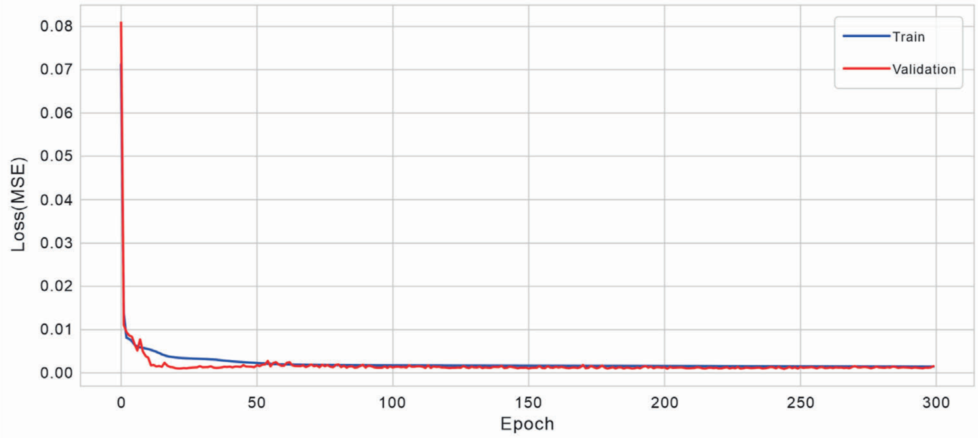

Fig. 11. The training and validation loss of the LSTM-AE model.

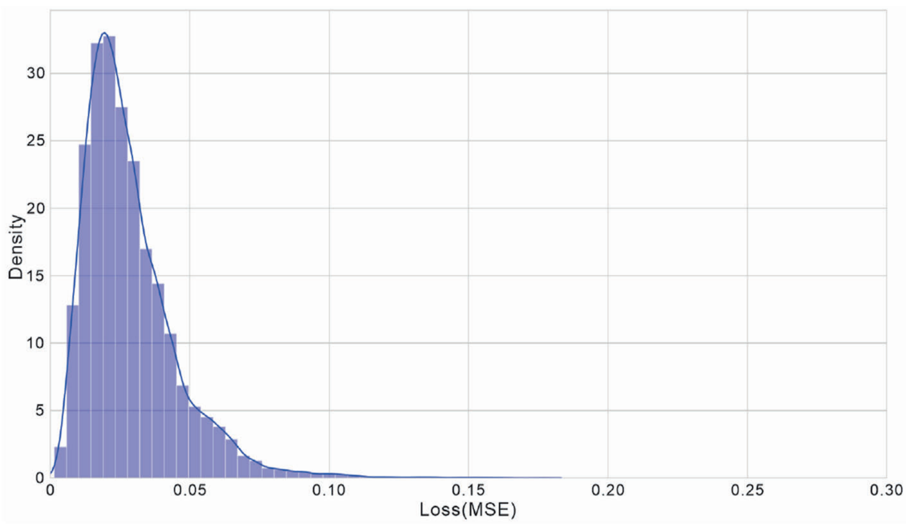

Fig. 12. The loss distribution plot.

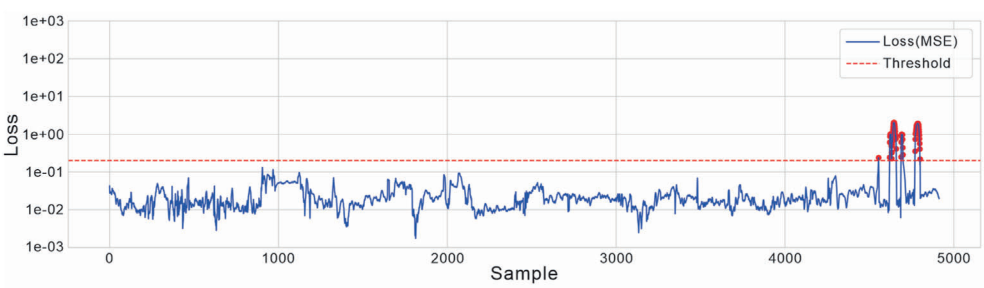

Fig. 13. The anomaly detection results for the test set.

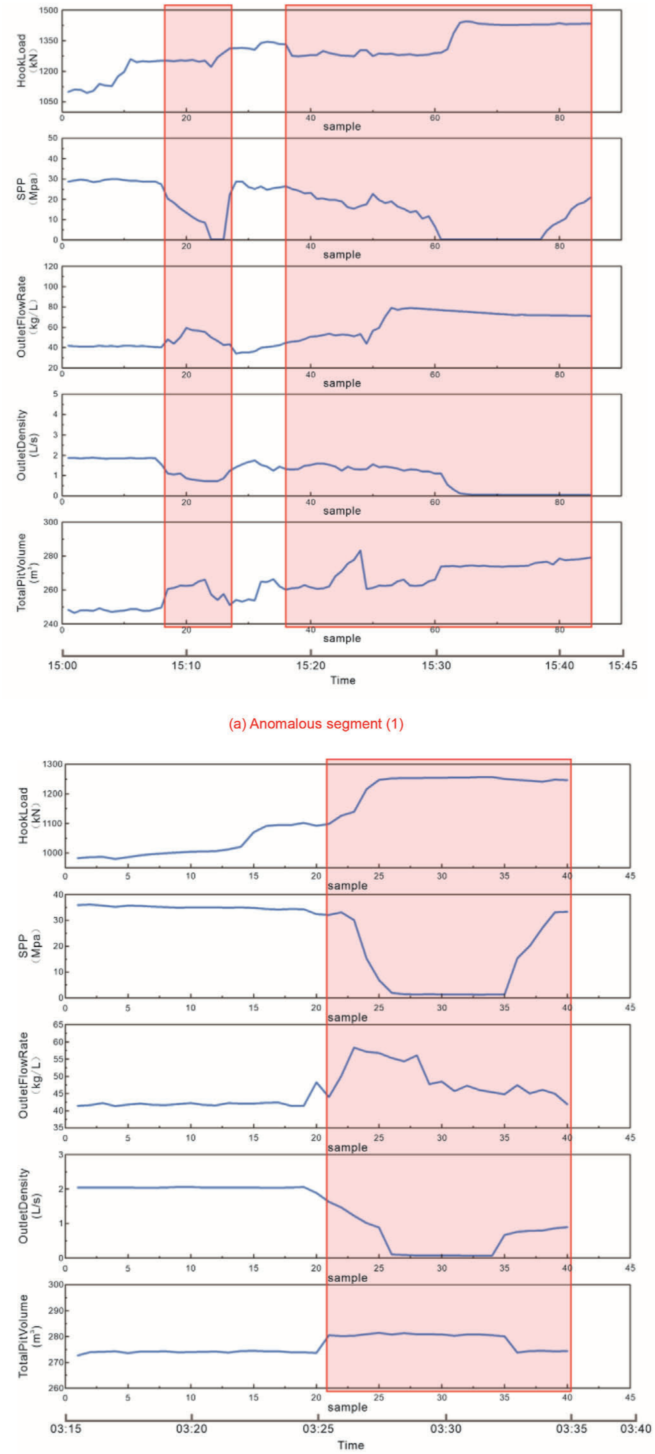

(a) Anomalous segment (1)

(b) Anomalous segment (2)

Fig. 14. The trend curves for the variation of each paramete from Well L58XX-X (with the anomalous segment highlighted in red).

data points, 83 were identified as anomalies. Upon cross-referencing with the original data, it was confirmed that there were four significant data fluctuations during this time period, and these fluctuations closely matched the detected anomalies.

3.2. Case studies

This section uses the intelligent kick early warning system to validate the results with field data. The field is located in the southern Sichuan Basin. This area has undergone a transition from marine to continental sedimentation, resulting in complex structural deformation characteristics. The overall characteristics of the work area include intense folding deformation, multi-phase and multi-scale fracture distribution, and significant differences in the lithology and thickness of the overlying strata, leading to a complex vertical pressure system. When drilling through areas with developed fractures or karst caves, fluid migration is likely to occur, leading to kick. Therefore, the difficulty of downhole accident risk warning is high in this region.

A. Well L58XX-X

The data for this well was collected at 30-s intervals. Fig. 14 shows the raw data of the anomalous segment of Well L58XX-X.

Fig. 15 shows the detection results for a specific segment of Well L58XX-X.

In Fig. 14(a), data from 15:00 to 15:48 on a certain day. According to the well history, the well depth was approximately 2908 m at this time. Personnel noticed a slight kick at 15:12, stopped pumping for 2 min, and then resumed drilling. At 15:30, they observed an increase in kick, prompting an emergency shutdown of the well. Pressurized well control was completed by 15:41, and pumping resumed for drilling. The figure indicates that the warning system detected an abnormal fluctuation at the 19th data point (15:08). Further analysis based on the proposed kick judgment rules confirmed kick occurrence between 15:08 and 15:14, which was 4 min earlier than manual detection. At the 34th data point (15:18), another abnormal fluctuation was detected. According to the rules, this kick period was determined to be from 15:18 to 15:43, which was 12 min earlier than manual detection. At the point of kick termination, there was a sudden change in data due to the completion of pressurized well control and resumption of pumping. However, the values still conformed to the kick rules, resulting in the identified abnormal segment being longer, and the kick segment being extended by 2 min.

In Fig. 14(b), data from 03:00 to 03:40 on a certain day. The well history indicates that the well depth in this section was approximately 4110 m. At 03:30, personnel observed kick and subsequently shut down the pump and well. Pressurized well control was completed by 03:41, and pumping resumed for drilling. The warning system detected an anomaly at the 21st data point (03:25). Further analysis based on the proposed kick judgment rules confirmed kick occurrence between 03:26 and 03:44, which was 4 min earlier than manual detection. In the termination point judgment, due to the pump resumption causing data fluctuations in this segment, the warning system extended the kick termination warning time by 3 min.

B. Well P6XX-X

The data for this well was collected at approximately 6-s intervals. Fig. 16 shows the raw data of the anomalous segment of Well P6XX-X.

Fig. 17 shows the detection results for the kick segment of Well P6XX-X.

According to the well history data, the well depth at this segment was 4396 m. On a certain day at 18:40, field staff detected a kick, stopped the pump, and shut down the well. Drilling

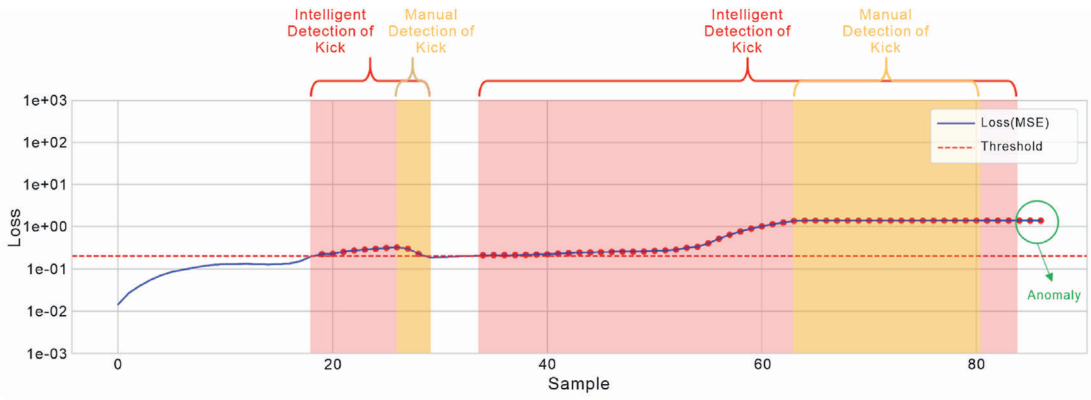

(a) Detection result of Segment (1).

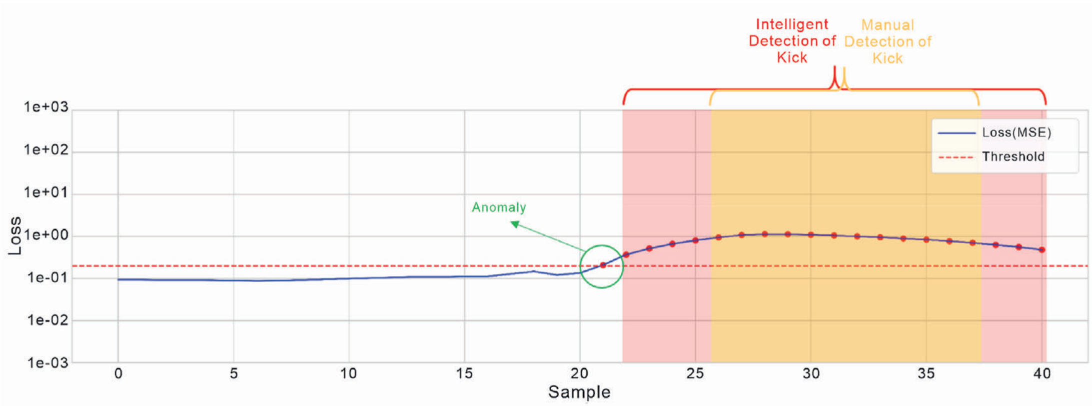

(b) Detection result of Segment (2).

Fig. 15. Detection result of partial drilling data for Well L58XX-X.

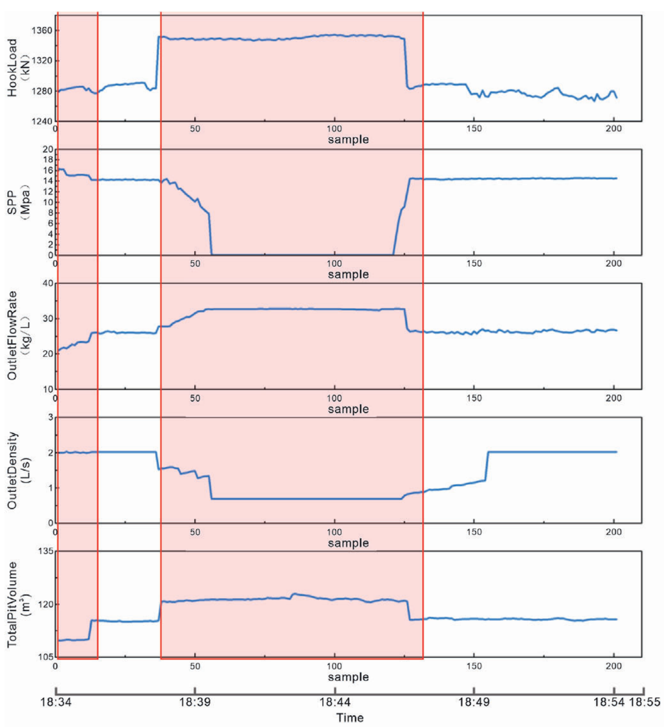

Fig. 16. The trend curves for the variation of each paramete from Well P6XX-X (with the anomalous segment highlighted in red).

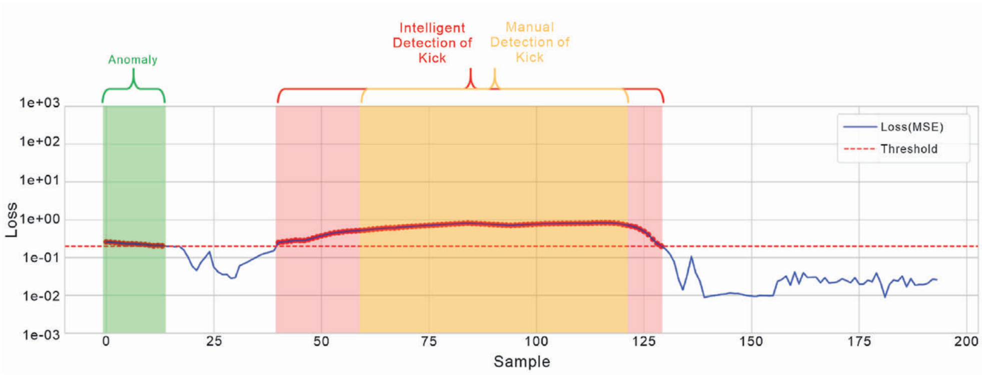

Fig. 17. Detection result of partial raw data for Well P6XX-X.

Table 3
Performance comparison of 6 models.

Well Name	Model	False alarm rate (%)	Average time of earlier warning (min)
L58XX-X	BP (Yin et al., 2014)	10.13	1
	LSTM (Wang et al., 2022,b)	9.34	5
	LSTM-RNN (Wang et al., 2023)	6.77	7
	AE (Vasafi et al., 2021)	5.21	4
	LSTM-AE(Ours)	**4.18**	**10**
	SAE (Zhang et al., 2023b)	4.32	8
P6XX-X	BP	14.68	1
	LSTM	9.21	3
	LSTM-RNN	6.63	6
	AE	5.11	6
	LSTM-AE(Ours)	**4.23**	**9**
	SAE	4.19	9
S21X-X	BP	13.15	2
	LSTM	9.87	5
	LSTM-RNN	7.54	7
	AE	6.13	5
	LSTM-AE(Ours)	**4.39**	**8**
	SAE	4.51	6
Y6X-X	BP	15.11	1
	LSTM	10.95	3
	LSTM-RNN	9.44	6
	AE	7.45	5
	LSTM-AE(Ours)	**5.04**	**9**
	SAE	5.39	7
F7X-X	BP	14.36	1
	LSTM	10.20	2
	LSTM-RNN	8.37	4
	AE	8.05	4
	LSTM-AE(Ours)	**4.96**	**10**
	SAE	5.17	7

resumed after 18:45. The system identified two segments of anomalous fluctuations in this period. According to the kick detection rules, the monitoring system detected a minor kick starting from the 40th data point (18:38) and ended the warning at 18:47. This warning was issued 2 min earlier than the manual warning, although the warning end time was delayed by 2 min due to fluctuations from the resumed drilling data. Anomalies detected from the first data point did not meet the criteria for a kick after applying the rules.

3.3. Discussion and evaluation

Verification with field data confirms that the intelligent kick early warning system, comprised of the LSTM-AE model and kick detection rules, effectively monitors and warns for kicks. Detection results for the kick segments in Well L58XX-X and Well P6XX-X demonstrate that the system is sensitive to data changes, accurately detecting anomalous sequences, and capable of identifying minor kick with short durations. The system can also switch warning states rapidly. In Fig. 17, the first segment of anomalies was not identified as a kick, whereas the well history data indicates a loss occurred in that segment. This suggests that when the detection rules meet specific conditions, it is feasible to use the anomaly sequence to identify other downhole incidents. Moreover, the system provides advanced warnings, with all three kick segments detected earlier than manual warnings. However, the system showed a slight delay in ending the warnings compared to manual detection. This issue can be addressed by adding a shut-in signal in the software. When the well is shut in, this signal could guide the system to switch states and end the warning appropriately.

In kick detection task, where the number of normal samples is vast and kick samples are scarce. In imbalanced datasets, metrics such as accuracy, precision, and recall often fail to effectively measure a model's performance. In anomaly detection, the model may perform poorly in identifying the minority class, but due to its good performance on the majority (normal) class, the overall accuracy can still appear high. This can obscure the model's poor

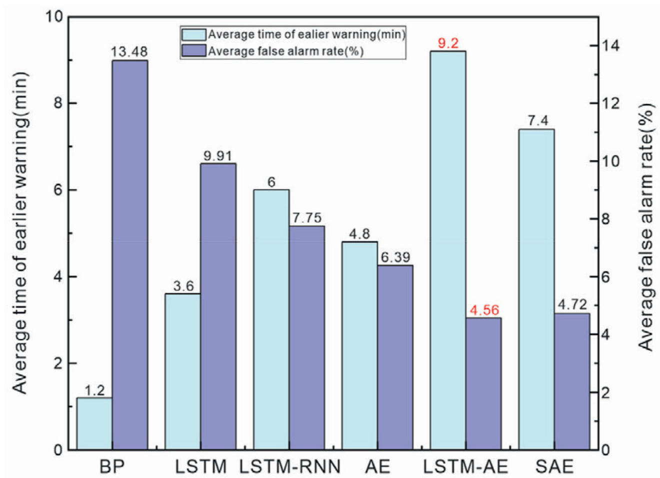

Fig. 18. Average performance metrics of the 6 models.

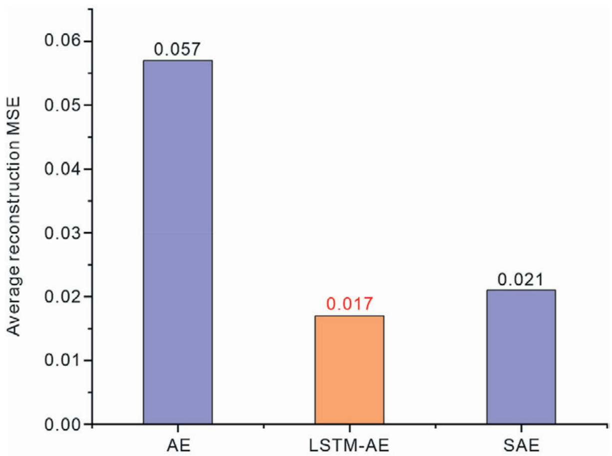

Fig. 19. Average reconstruction MSE of 3 models.

Table 4
Training time for 6 models at convergence.

Model	Training Dataset size	Validation Dataset size	Convergence Epoch	Convergence time (s)
BP	28576	5715	100	83
LSTM			120	95
LSTM-RNN			160	114
AE			80	45
LSTM-AE (Ours)			**100**	**65**
SAE			90	57

performance in detecting the minority class. Additionally, each false alarm in drilling operations necessitates a halt for inspection, leading to reduced operational efficiency and substantial economic losses. Therefore, this paper adopts the false alarm rate as the model evaluation metric. Its calculation formula is as follows:

$$R_{False} = \frac{N_{FN}}{N_{FN} + N_{TP}} \times 100\% \tag{10}$$

where N_{FN} is the number of time sequences incorrectly detected as kick under normal conditions; N_{TP} is the number of time sequences correctly detected as kick under normal conditions. According to this metric, the paper conducted kick detection on data from five wells using three common supervised learning methods and two autoencoder methods. The comparative results are presented in Table 3 and Fig. 18.

From Table 3 and Fig. 18, it can be seen that the LSTM-AE model has an average false alarm rate of 4.56% across five wells and detects kicks an average of 9.2 min earlier than manual detection. Among the six models evaluated, it exhibits the best performance. These results demonstrate the effectiveness of the proposed method, showing that its performance is superior to that of supervised learning methods and traditional autoencoders (AE, SAE).

Regarding the model transferability, Fig. 19 displays the average mean squared error of reconstruction for normal drilling data from five wells using the three unsupervised learning models. The average MSE of reconstruction for LSTM-AE is 0.017, indicating superior generalization ability compared to AE and SAE. This makes it more suitable for use across different well sites in various blocks.

The training time of the model is influenced by the computer configuration, as well as the scale and complexity of the dataset. The test machine used for this evaluation is equipped with an Intel Core i7-10700F CPU, 16 GB of RAM, and an NVIDIA GeForce RTX 2060 SUPER 8 GB GPU. Using this test machine, we conducted model training time tests with the same dataset, and the results are shown in Table 4.

From the analysis of Tables 4 and it can be observed that the LSTM-AE model converges faster than supervised learning methods, with little difference in convergence time compared to AE and SAE. In practical applications, models are typically trained on offline data before being deployed, so the minor differences in training time do not impact normal operations.

4. Conclusion

(1) This paper proposes an intelligent kick early warning method based on unsupervised learning. The training of this model does not rely on labeled samples, thus avoiding the issue of class imbalance in the training set.
(2) The intelligent kick early warning platform combines an LSTM-AE-based drilling sequence anomaly detection model with expert knowledge-based kick warning rules. This platform was validated with field data from five wells and compared with other intelligent kick detection methods. The experimental results indicate that this method achieves early kick detection with a low false alarm rate. The performance metrics of LSTM-AE surpass those of BP, LSTM, and LSTM-RNN, which are supervised learning methods, and the model's generalization ability also exceeds that of AE and SAE. This confirms that unsupervised learning can effectively improve the accuracy and generalization ability of the model. Moreover, LSTM-AE is more suitable for drilling data and can provide effective technical support for oil and gas drilling safety.
(3) In the application to Well P6XX-X, the anomaly segment not identified as a kick closely matched the loss segment recorded in the well history. This demonstrates that the intelligent kick detection method, which combines the model and judgment rules, is also significant for the intelligent identification of other downhole incidents.

Based on the model proposed in this paper, future work will focus on expanding the application scope of the model and enhancing its transferability and generalization capabilities. This includes developing specialized models for different complex downhole incidents and constructing a system capable of identifying multiple incidents through ensemble learning. By leveraging cloud databases and federated learning, the transferability of the model can be improved while ensuring data security. These measures aim to further enhance the model's performance and application range in intelligent early warning, providing stronger technical support for oil and gas drilling safety.

CRediT authorship contribution statement

Boyuan Li: Writing – review & editing, Writing – original draft, Visualization, Validation, Methodology, Investigation. **Zhaoxue Guo:** Writing – review & editing, Validation, Supervision, Resources, Funding acquisition. **Xudong Wang:** Supervision, Software, Resources, Investigation. **Gui Tang:** Validation, Resources, Funding acquisition. **Xing Zuo:** Validation, Supervision, Resources.

Declaration of competing interest

The authors declare that they have no known competing financial interests or personal relationships that could have appeared to influence the work reported in this paper.

Acknowledgments

This work is financially supported by the Industrial Project “Intelligent Pressure Control Drilling Technology Based on Data-Driven Approach” from CNPC Chuanqing Drilling & Production Engineering Technology Research Institute, and also benefits from the experimental conditions provided on site. The authors would also like to thank Engineer Yulin Liang of CNPC Chuanqing Drilling Engineering Co., Ltd. for providing the data support.

Nomenclature

LSTM-AE	Long short-term memory autoencoder
SDM	Smart drillpipe monitoring
MWD	Measurement while drilling
AI	Artificial intelligence
BN	Bayesian network
KNN	K-nearest neighbors
SVM	Support vector machines
BSMOTE-SVM	Borderline smote-support vector machines
BP	Backpropagation neural network
RNN	Recurrent neural network
CNN	Convolutional neural network
GA	Genetic algorithm
ANN	Artificial neural network
GA-BP	Genetic algorithm-Backpropagation
CPSO-BP	Cognitive particle swarm optimization-Backpropagation
LSTM	Long short-term memory
BiLSTM	Bidirectional long short-term memory
GRU	Gated recurrent unit
BiGRU	Bidirectional gated recurrent unit
LSTM-RNN	Long short-term memory-Recurrent neural network
AE	Autoencoder
SAE	Spares autoencoder
RNN-AE	Recurrent neural network autoencoder
CNN-AE	Convolutional neural network autoencoder
OSAVA	Orthogonal self-attentive variational autoencoder
SPP	Standpipe pressure
ROP	Rate of penetration
MSE	Mean-square error
KDE	Kernel density estimation

References

Agostini, C.E., Sampaio, M.A., 2020. Probabilistic Neural Network with Bayesian-based, spectral torque imaging and Deep Convolutional Autoencoder for PDC bit wear monitoring. J. Petrol. Sci. Eng. 193, 107434.

Ahmed, M.A., Hegab, O.A., Sabry, A., 2016. Early detection enhancement of the kick and near-balance drilling using mud logging warning sign. Egyptian J Basic Appl Sci 3 (1), 85–93.

Alouhali, R., Aljubran, M., Gharbi, S., Al-Yami, A., 2018. Drilling through data: automated kick detection using data mining. In: SPE International Heavy Oil Conference and Exhibition.

Al-Yami, A.,S., Al-Shaarawi, A., Al-Bahrani, H., 2016. Using bayesian network to develop drilling expert systems. In: SPE Heavy Oil Conference and Exhibition.

Andia, P., Israel, R.R., 2018. A cyber-physical approach to early kick detection. In: The IADC/SPE Drilling Conference and Exhibition.

Arunthavanathan, R., Khan, F., Ahmed, S., Imtiaz, S., 2021. An analysis of process fault diagnosis methods from safety perspectives. Comput. Chem. Eng. 145, 107197.

Bi, X., Zhao, J., 2021. A novel orthogonal self-attentive variational autoencoder method for interpretable chemical process fault detection and identification. Process Saf. Environ. Prot. 156, 581–597.

Fjetland, A.K., Zhou, J., Abeyrathna, K.D., Gravdal, J.E., 2019. Kick detection and influx size estimation during offshore drilling operations using deep learning. In: IEEE Conference on Industrial Electronics and Applications.

Fu, J., Su, Y., Jiang, W., Xu, L., 2015. Development and testing of kick detection system at mud line in deepwater drilling. J. Petrol. Sci. Eng. 135, 452–460.

Ge, L., Teng, Y., Xiao, Q., Xiao, X., Deng, H., 2023. Research on overflow intelligent warning technology based on downhole annulus parameters. J Southwest Petr Univer (Sci; TechnolEd) 45 (2), 126–134.

Greff, K., Srivastava, R.K., Koutnik, J., Steunebrink, B.R., Schmidhuber, J., 2017. LSTM: a search space odyssey. IEEE Transact. Neural Networks Learn. Syst. 28 (10), 2222–2232.

Hargreaves, D., Jardine, S., Jeffryes, B., 2001. Early kick detection for deepwater drilling: new probabilistic methods applied in the field. In: SPE Annual Technical Conference and Exhibition.

He, T., Zhang, Z., Zhang, H., Zhang, Z., Xie, J., Li, M., 2019. Bag of tricks for image classification with convolutional neural networks. In: 2019 IEEE/CVF Conference on Computer Vision and Pattern Recognition (CVPR).

Isemin, I.A., Nkundu, K.A.B., Agwu, O.E., 2019. Utilization of big data analytics and advanced formation modelling for detection of kicks in drilling operations. In: The SPE Nigeria Annual International Conference and Exhibition.

Islam, R., Khan, F., Venkatesan, R., 2017. Real time risk analysis of kick detection: testing and validation. Reliab. Eng. Syst. Saf. 161, 25–37.

Kingma, D.P., Ba, J., 2015. Adam: a method for stochastic optimization. In: The 3rd International Conference for Learning Representations arXiv: 1412.6980.

Konda, R.M., Hakan, B., Naoki, T., Ryota, W., Tomoya, I., Kazuya, K., Tazuru, N., Hitoshi, T., 2022. Early sign detection for the stuck pipe scenarios using unsupervised deep learning. J. Petrol. Sci. Eng. 208, 109489.

Kopbayev, A., Khan, F., Yang, M., Halim, S.Z., 2022. Gas leakage detection using spatial and temporal neural network model. Process Saf. Environ. Prot. 160, 968–975.

Li, H.Y., Tan, Q., Li, B., Feng, Y., Dong, B., Yan, K., Ding, J., Zhang, S., Guo, J., Deng, J., 2023. Physically-data driven approach for predicting formation leakage pressure: a dual-drive method. Appl. Sci. 13 (18), 10147.

Li, H., Man, Y., Li, H., 2023. Research on kick warning based on relative entropy improved fuzzy C-mean clustering. Drill. Prod. Technol. 46 (3), 165–170.

Li, T., 2021. Research on Prediction of Downhole Stuck Pipe Based on Neural Network. Xi'an Shiyou University, China.

Li, X., Zhang, J., Tang, X., Li, C., Li, B., Wang, Y., Zhao, Z., 2022. Propagation characteristics and application effects of measurement-while-drilling pressure wave for early gas-kick detection. J. Loss Prev. Process. Ind. 76, 104741.

Li, Y.J., 2020. Research and Application of Drilling Risk Monitoring Method Based on Expert System and Long short-term Memory Network. China University of Petroleum (East China).

Ma, T.S., Xiang, G.F., Gui, J.C., Jia, L.C., Tang, Y.J., 2024. Physics-constrained distributed neural network model for 3D in-situ stress prediction. Chin. J. Geophys. 67 (8), 3211–3228.

Mason, C.F., 2019. Policy brief-gulating offshore oil and gas exploration: insights from the deepwater horizon experience in the Gulf of Mexico. Rev. Environ. Econ. Pol. 13 (1), 149–154.

Muojeke, S., Venkatesan, R., Khan, F., 2020. Supervised data-driven approach to early kick detection during drilling operation. J. Pet. Sci. Eng. 192, 107324.

Nayeem, A.A., Venkatesan, R., Khan, F., 2016. Monitoring of down-hole parameters for early kick detection. J. Loss Prev. Process. Ind. 40, 43–54.

Nhat, D.M., Venkatesan, R., Khan, F., 2020. Data-driven Bayesian network model for early kick detection in industrial drilling process. Process Saf. Environ. Prot. 138, 130–138.

Obi, C.E., Falola, Y., Manikonda, K., Hasan, A.R., Rahman, M.A., 2022. Flow pattern, pressure gradient relationship of gas kick under dynamic conditions. In: The Offshore Technology Conference.

Osarogiagbon, A., Khan, F., Venkatesan, R., Gillard, P., 2021. Review and analysis of supervised machine learning algorithms for hazardous events in drilling operations. Process Saf. Environ. Prot. 147, 367–384.

Osarogiagbon, A., Muojeke, S., Venkatesan, R., Khan, F., Gillard, P., 2020. A new methodology for kick detection during petroleum drilling using long short-

term memory recurrent neural network. Process Saf. Environ. Prot. 142, 126–137.
Park, J., Jeong, J., 2023. Assessment of the effectiveness of a convolutional autoencoder for digital image-based automated core logging. Geoenergy Sci. Eng. 227, 211802.
Ritchie, G.M., Hutin, R., Aldred, W.D., Luppens, J., 2008. Development and testing of a rig-based quick event detection system to mitigate drilling risks. In: IADC/SPE Drilling Conference.
Shi, X., Cui, M., Ji, Y., Wu, D., Guo, W., Jing, L., Tian, Y., Yang, X., 2023. Novel Kick detection tool based on knowledge-data-dual-driven approaches. In: The SPE Offshore Europe Conference & Exhibition.
Su, Y., Ma, H., Guo, J., Shen, X., Yang, Z., Wu, J., 2024. The behaviors of gas-liquid two-phase flow under gas kick during horizontal drilling with oil-based muds. Petroleum 10, 49–67.
Sule, I.O., Khan, F., Butt, S., 2019. Experimental investigation of gas kick effects on dynamic drilling parameters. J. Pet. Explor. Prod. Technol. 9 (1), 605–616.
Sun, W., Liu, K., Zhang, D., Li, W., Xu, L., Dai, Y., 2023. A kick and lost circulation monitoring method combining Bi-GRU and drilling conditions. Petr. Drill. Techn. 51 (3), 37–44.
Sun, X., Sun, B., Zhang, S., Wang, Z., Gao, Y., Li, H., 2018. A new pattern recognition model for gas kick diagnosis in deepwater drilling. J. Petrol. Sci. Eng. 167, 418–425.
Tan, B., Zhang, B., Tao, H., 2024. Current situation and development of deep exploration key drilling technology. Drill. Prod. Technol. 47 (2), 70–82.
Vasafi, P.S., Paquet-Durand, O., Brettschneider, K., Hinrichs, J., Hitzmann, B., 2021. Anomaly detection during milk processing by autoencoder neural network based on near-infrared spectroscopy. J. Food Eng. 299, 110510.
Wang, J., Ozbayoglu, E., Baldino, S., Liu, Y., Zheng, D., 2023. Time series data analysis with recurrent neural network for early kick detection. In: Offshore Technology Conference.
Wang, Y., Hao, J., Zhang, F., Wei, Q., Peng, Z., Duan, M., 2022a. Adaptive LSTM early warning method for kick detection in drilling. Control Theory Appl. 39 (3), 441–448.
Wang, Z., Chen, G., Zhang, R., Zhou, W., Hu, Y., Zhao, X., Wang, P., 2022b. Early monitoring of gas kick in deepwater drilling based on ensemble learning method: a case study at South China Sea. Process Saf. Environ. Prot. 169, 504–514.
Xie, H., Shanmugam, A.K., Issa, R.R.A., 2018. Big data analysis for monitoring of kick formation in complex underwater drilling projects. J. Comput. Civ. Eng. 32 (5), 04018030.1-04018030.11.
Xu, Y., Liu, K., He, B., Pinyaeva, T., Li, B., Wang, Y., Nie, J., Yang, L., Li, F., 2023. Risk pre-assessment method for regional drilling engineering based on deep learning and multi-source data. Pet. Sci. 20 (6), 3654–3672.
Yang, H., Li, J., Liu, G., Wang, C., Wang, B., 2019. A new method for early gas kick detection based on the consistencies and differences of bottomhole pressures at two measured points. J. Pet. Sci. Eng. 176, 1095–1105.
Yin, H., Si, M., Wang, H., 2014. The warning model of the early kick based on BP neural network Pakistan. J. Stat. 30 (6), 1047–1056.
Yin, Q., Song, Z., Chen, K., Zhou, X., Tyagi, M., Li, L., 2023. Early warning of deep-water drilling influx based on machine learning. In: The 33rd International Ocean and Polar Engineering Conference.
Yue, W., 2014. Design and Development of Online Monitoring and Early Warning System for “Three High” Oil and Gas Well Blowout Precursor. China University of Petroleum, China (East China).
Zhang, D., Sun, W., Dai, Y., Liu, K., Li, W., Wang, C., 2023. A hierarchical early kick detection method using a cascaded GRU network. Geoenergy Sci. Eng. 222, 211390.
Zhang, H., Chi, Z., 2023. Kick risk assessment based on BSMOTE-SVM algorithm. Control Eng. China 30 (12), 2173–2178.
Zhang, H., Li, Q., Zhang, L., Mi, L., 2016. Intelligent warning technology for drilling overflow based on fuzzy expert system. J Southwest Petr Univer (Sci; TechnolEd) 38 (2), 169–175.
Zhang, S., Samuel, R., 2024. Advanced realtime early kick and loss detection (EKLD) through a hybrid data-driven and physics-constrained approach. In: The SPE Western Regional Meeting.
Zhang, Z., 2014. Research on Abnormal Warning Methods in Drilling Engineering. Southwest Petroleum University, China.
Zhang, Z., Lai, X., Du, S., Yu, W., Wu, M., 2023b. Early warning of loss and kick for drilling process based on sparse autoencoder with multivariate time series. IEEE Trans. Ind. Inf. 19 (11), 1–11.
Zhang, Z., Zhao, Y., Wang, J., Wang, G., Zhong, L., Lu, J., Yuan, J., 2023a. A real time monitoring method for well-kick and lost circulation based on distributed fiber optic temperature measurement. Geoenergy Sci. Eng. 229, 212087.
Zhao, Y., Huang, Z., Xin, F., Qi, G., Huang, H., 2022. Kick prediction method based on artificial neural network model. Energies 15 (16), 5912.
Zhu, H., Wang, S., Li, Z., Yan, X., Gong, P., 2019. A new high-precision timely monitoring and metering system for early kick and loss. Nat. Gas. Ind. B 6 (4), 394–398.